Stefania Sabella[1]
Milena Quaglia[1, 2]
Cristina Lanni[3]
Marco Racchi[3]
Stefano Govoni[3]
Gabriele Caccialanza[1]
Alberto Calligaro[4]
Vittorio Bellotti[2]
Ersilia De Lorenzi[1]

[1]Department of Pharmaceutical Chemistry, School of Pharmacy
[2]Biotechnology Laboratories, IRCCS, S. Matteo Hospital – Department of Biochemistry, School of Pharmacy
[3]Department of Experimental and Applied Pharmacology, School of Pharmacy
[4]Department of Experimental Medicine, Histology and Embriology Unit, School of Medicine, University of Pavia, Pavia, Italy

Capillary electrophoresis studies on the aggregation process of β-amyloid 1-42 and 1-40 peptides

The possibility to monitor, in solution, the steps of β-amyloid (Aβ) nucleation and therefore to describe this dynamic process by using capillary electrophoresis and under optimized experimental conditions is described. Striking differences in the electrophoretic patterns of Aβ 1-42 and Aβ 1-40 over time are here shown, and different aggregation states are elucidated, which reflect the very diverse oligomerization behavior of two very similar peptides. The isolation of one aggregated species of high molecular weight by ultracentrifugation allowed us to assess its role as toxic oligomer. The perturbation of the existing equilibrium among the identified species by the addition of small molecules can in principle interfere with the aggregation process of the peptides and ultimately prevent the plaque formation *in vitro*.

Keywords: Alzheimer's disease / β-Amyloid / Capillary electrophoresis
DOI 10.1002/elps.200406062

1 Introduction

It is well known that protein folding abnormalities are recognized to be responsible for diseases like amyloidosis and neurodegenerative disorders associated to accumulation of fibrillar proteins like Parkinson's and Alzheimer's disease [1, 2]. All these pathologies share the presence of a partially structured protein or of peptide conformers that slowly deposit in insoluble polymeric aggregates named fibrils.

β-Amyloid (Aβ) peptides involved in Alzheimer's disease derive from the proteolytic processing of a larger amyloid precursor protein and in particular Aβ 1-42 and Aβ 1-40, composed of 42 and 40 amino acids, respectively, play an important role in the etiology of the disease. These peptides are normally present in human plasma and cerebrospinal fluid [3, 4], but under pathological conditions, they aggregate and form fibrils which accumulate in the brain as inert and diffuse plaques [5]. Recent studies have shown that fibrillogenesis from Aβ 1-42 and Aβ 1-40 monomers occurs through the formation of partially folded conformers which are globular monomeric assemblies at different aggregation phases, and protofibrils, which seem to be the major effectors of the neurotoxicity [6, 7].

Spectroscopic studies have demonstrated that in the oligomerization process Aβ 1-42 and Aβ 1-40 are subjected to conformational changes. NMR investigations evidenced that transitory conversion of the random coil monomer structure into a predominant helical structure occurs [8, 9], and this evidence has been confirmed by circular dicroism, where it was possible to observe that soluble oligomers, that represent early intermediates of the fibrillogenic pathway, display a significant percentage of α-helix [10]. As the formation of the α secondary structure is a key step of the aggregation process, a nucleation-elongation mechanism has been proposed [11], where the oligomer formation takes place through the agglomeration of α-helix rich nuclei or seeds [10, 12].

One of the most difficult tasks in this field is represented by the development of techniques suitable for the investigations in real time of the fibrillogenic process and for the correlation of the association state with one of the most intrinsic functions assigned to the oligomers, like the cytotoxic activity. By size-exclusion chromatography, Roher *et al.* [13] described the oligomeric distribution of Aβ peptides in the first stage of aggregation and observed

Correspondence: Prof. Ersilia De Lorenzi, Department of Pharmaceutical Chemistry, University of Pavia, Viale Taramelli 12, I-27100 Pavia, Italy
E-mail: ersidelo@unipv.it
Fax: +39-0382-422975

Abbreviations: Aβ, β-amyloid; **HFIP**, 1,1,1,3,3,3-hexafluoro-2-propanol; **MTT**, 3-(4,5-dimethylthiazol-2-yl)-2,5-diphenyl-tetrazolium bromide

that Aβ 1-42 and Aβ 1-40 are present in monomeric, dimeric and trimeric forms whose presence increases with the time of incubation.

The quantitative kinetic description of this process has been demonstrated to be awkward, as these peptides are very unstable and furthermore *in vitro* studies are extremely susceptible to sample preparation and experimental conditions. LaDu *et al.* [14, 15] reported two protocols to start from monomers or low-molecular-weight oligomers and produce fibrils *in vitro,* also monitoring by atomic force microscopy and SDS-PAGE the aggregation behavior under different experimental conditions (pH, temperature, time of incubation, concentrations, *etc.*). By a photoinduced covalent cross-linking, Bitan *et al.* [16] have managed to "freeze" some aggregation states by stabilizing the oligomers, and by using this approach it was possible to characterize the oligomers related to a certain state of aggregation [17]. This seminal study evidenced that Aβ 1-42 preferentially forms pentameric and hexameric oligomers (paranuclei) that associate to larger oligomers and protofibrils, thus confirming a nucleation-elongation mechanism. Conversely, Aβ 1-40 does not seem to generate such paranuclei and undergoes a slower aggregation process compared to that of Aβ 1-42 [17].

In the present work, we used capillary electrophoresis to combine the electrophoretic separation principles with the ability to give a real snapshot of the population of oligomers during their formation. No covalent modification to stabilize the oligomers was carried out, so to monitor the fibrillogenic process under conditions that do not affect the structural dynamics of the oligomer and at a pH value as much as possible similar to that of plasma and of the cerebrospinal fluid. This approach allowed the comparison of the electrophoretic results with the cytotoxic activity of the oligomers on the cells. CE offers a high potential, as it allows for a dynamic monitoring, in aqueous solution and under mild conditions, of Aβ 1-40 and Aβ 1-42 nucleation steps. The minimum material consumption, the possibility of automation and short analysis times are most valuable assets in this context. To our knowledge, CE has been so far used only for the quantitative analysis of Aβ 1-40 in biological fluids when coupled to mass spectrometry [18] and for the determination of the enantiomeric composition of the same peptide by MEKC-LIF [19]. Here, we exploit the separation potential of CE and of the ultrafiltration technique to describe the oligomer population of Aβ 1-42 and Aβ 1-40 along the fibrillogenic pathway and to isolate a high-molecular-weight oligomer peak that is found to correspond to the toxic species of Aβ 1-42.

2 Materials and methods

2.1 Chemicals

Aβ 1-42 was synthesized at the Core Protein Laboratory of Wake Forest University (Dr. M. O. Lively) and Aβ 1-40 was kindly donated by Pharmacia (Nerviano, Italy), respectively. NaH_2PO_4, Na_2HPO_4, Na_2CO_3 were provided by Merck (Darmstadt, Germany). 1,1,1,3,3,3-Hexafluoro-2-propanol (HFIP) was supplied by Sigma (St. Louis, MO, USA) and DMSO by Carlo Erba Reagenti (Milan, Italy). Microcon Centrifugal Filter Devices (Microcon YM-3, YM-10, YM-30, YM-50) from Millipore (Bedford, MA, USA) were used for the characterization studies. Water was deionized by passing through a Direct-Q™ Millipore system (Bedford, MA, USA).

2.2 Sample preparation

Procedure A: Aβ 1-40 and Aβ 1-42 were dissolved in acetonitrile/300 μM Na_2CO_3 pH 10.5 (50:50 v/v), to obtain a final sample concentration of 100 μM. The acetonitrile/Na_2CO_3 mixture was chosen in order to obtain a readily soluble peptide at the operative concentration. Basic pH is intended to increase the solubility of acidic Aβ peptides and Na_2CO_3 rather than NaOH was used to avoid damage of either the peptides or the neuroblastoma cells. Na_2CO_3 concentration was chosen on the basis of stoichiometric calculations. The solutions were separated in aliquots, freeze-dried and stored at −20°C. The samples were then dissolved in 100 μL phosphate buffer (20 mM, pH 7.4) to obtain a final concentration of 100 μM and were sonicated for 3 min with an ultrasonic bath. After centrifugation (10 min at 14 437 × *g*), the supernatant was injected immediately (t_0) or kept at room temperature and injected at different elapsed times from withdrawal of the supernatant. For experiments with Microcon filters the supernatants were ultrafiltrated on Microcon filters with different cut-off values (3000, 10 000, 30 000, 50 000 Da) for 20 min at 14 437 × *g*. In order to obtain enough volume for injection and to approximately restore the original concentration, 80 μL of 20 mM phosphate buffer pH 7.4 was added to the retained sample, recovered by reverse spinning. Appropriate studies to quantify the retained sample amount were not carried out. However, the comparison between the electropherograms obtained before and after filtration indicate that the concentrations of the species injected in the CE system are comparable. The solutions (retained and filtrated) were immediately injected into the CE instrument or diluted 1:10 when used for cytotoxicity studies. Procedure B: A second lyophilization procedure was carried out for Aβ 1-40 by slightly modifying the procedure described by LaDu *et al.* [14]. Aβ 1-40

was dissolved in 1 mM HFIP, freeze-dried and stored at −80°C. Immediately prior to use, the sample was dissolved in DMSO to obtain a concentration of 5 mM, divided in two aliquots and diluted to 100 μM by using either phosphate buffer (20 mM, pH 7.4) or HCl (30 mM, pH 1.6), respectively. The samples were sonicated for 3 min, centrifuged at 14 437 × *g* for 10 min and injected into the CE system.

2.3 Capillary electrophoresis

All experiments were performed on an Agilent Technologies 3D capillary electrophoresis system with built-in diode-array detector (Waldbronn, Germany). Data were collected and analyzed using an HP Vectra XA/166 computer utilizing a Chemstation A.10.01 software. Unless otherwise stated, the uncoated fused-silica capillary (50 μm ID, 53 cm total length, 48.5 cm to the window) was from MicroQuartz (München, Germany). By applying a pressure of 1 bar to the capillary inlet, a new capillary was pretreated with 1 M NaOH for 30 min, followed by water for 30 min and by the background electrolyte (80 mM phosphate buffer, pH 7.4) for 60 min. Phosphate buffer was prepared by mixing 80 mM solutions of analytical-grade dibasic sodium hydrogen phosphate and sodium dihydrogen phosphate to give the desired pH. The between-run rinsing cycle was carried out by pumping through the capillary 50 mM SDS [20] and water for 1.5 min each and running buffer for 2 min. The injection of the samples was carried out by applying a pressure of 50 mbar for 8 s. The capillaries were thermostated with circulating air at 25°C and separations, unless otherwise stated, were carried out at 16 kV (current = 77.2–77.9 μA) with the anode at the sample injection end. The wavelength was fixed at 200 nm. Buffer solutions were freshly prepared using deionized water. Prior to use, all solutions were filtered through a 0.45 μM Millipore membrane filter and degassed by sonication. The background electrolyte was prepared by mixing analytical-grade dibasic sodium hydrogen phosphate and sodium dihydrogen phosphate solutions, to give pH 7.4.

2.4 Cytoxicity studies

2.4.1 Cell cultures

IMR32 cell cultures (human neuroblastoma) were grown in RPMI 1640 medium containing 10% v/v fetal bovine serum, penicillin (100 U/mL), streptomycin (100 μg/mL), and 2 mM glutamine. Cells were maintained at 37°C in a humidified atmosphere of 5% CO_2 and 95% air. Materials used for cell cultures were obtained from Celbio (Milan, Italy).

2.4.2 Treatment and assessment of cell viability (MTT colorimetric assay)

The mitochondrial dehydrogenase activity that reduces 3-(4,5-dimethylthiazol-2-yl)-2,5-diphenyl-tetrazolium bromide (MTT, Sigma) was used to determine cellular redox activity, an initial indicator of cell death, in a quantitative colorimetric assay. At day 0, MR32 cells were plated at a density of 5×10^4 viable cells per well in 96-well plates. The next day, cells were incubated for 24 h at 37°C in the presence of Aβ 1-42 and Aβ 1-40. Cell viability was then evaluated using MTT colorimetric assay: MTT is an indicator of the mitochondrial activity of living cells. In the present study, cells were exposed to an MTT solution in PBS (1 mg/mL). Following 4 h incubation with MTT and treatment with SDS for 24 h, reduction into living cells was quantified by using a microplate reader Bio-Rad (Model 550; Hercules, CA, USA).

2.5 Electron microscopy

Negative staining of peptide solutions at concentrations of 100 μM was also performed. For each sample, a little drop (25 μL) of peptide solution was placed on a carbon-coated Formvar-covered copper grid (200 mesh). Sedimentation of peptide on the carbon film occurred during 2 min and negative staining was performed with a drop of 2% w/v uranyl acetate. The excess of staining solution was drained off by means of a filter paper and the specimen was transferred to the electron microscope for examination. Negatively stained samples were observed in a Zeiss EM 10 electron microscope operating at 80 and 100 kV at the magnifications of 40 000 and 63 000 ×. A 100 μm condenser aperture and a 50 μm objective aperture were used for the optimization of the resolution and the electronic contrast. Magnifications of the electron microscope were calibrated with a 2160 lines per millimeter diffraction grating replica onto 3.05 grids.

3 Results

3.1 Capillary electrophoresis

3.1.1 Aβ 1-42

Aβ 1-42 freeze-dried sample was treated according to procedure A reported in Section 2.2 and injected into the CE system immediately after withdrawal of the supernatant (t_0) (Fig. 1). A group of unresolved and fast migrating peaks (A) and a broad, slow migrating peak (B) were observed. Considering the high aggregation tendency of Aβ 1-42 to form oligomeric species in the fibrillogenic process [21], it is reasonable to think that these peaks

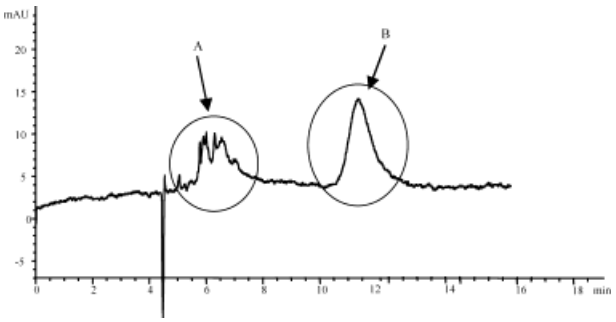

Figure 1. Electrophoretic profile of Aβ 1-42 immediately after supernatant withdrawal (t_0). Experimental conditions are given in Section 2.3.

could be representative of different oligomerization states of Aβ 1-42 monomers. Peak B has a slow electrophoretic mobility ($\mu_{eff} = -2.54 \times 10^{-4} \pm 2.22 \times 10^{-6}$; n=6) and it might conceivably be assigned as an oligomer of high molecular mass along the fibrillogenic pathway of the peptide.

No significant changes in the electrophoretic peak shapes and migration times were observed by injecting the peptide after different elapsed times from t_0, whereas the area of peak B clearly increases (Fig. 2). By plotting the normalized area of peak B and peak A [22], divided by the total peak areas, *vs.* the elapsed time from t_0 (Fig. 2, inset), it becomes evident that over the first 200 min peak B area increases very rapidly at the expenses of the area under the group of peaks named A, and further up to 24 h the extent of area variation is negligible (plateau). After 24 h and up to six days the electropherograms recorded remain unchanged. No peaks were instead detected at the seventh day from t_0 (data not shown) and this was attributed to sample precipitation and massive conversion into fibrillar aggregate, as the sample was visibly cloudy and electron microscopy disclosed the presence of non-branching fibrils presenting a diameter of 10 nm, consistent with the feature of classical amyloid fibrils [2] (Fig. 3).

In order to better characterize the electrophoretic peaks evidenced at t_0, samples of Aβ 1-42 were filtered and centrifuged by using different Microcon membranes, as indicated in Section 2.2. The filtrated (Fig. 4A) and the retained (Fig. 4B) solutions were injected into the CE and the electropherograms obtained were compared with that of Fig. 1 (here reported in the bottom lines, for clarity). All the peaks correspond to species characterized by molecular masses above 3000 Da. Species with molecular mass ranges of 3000–50 000 Da were found to correspond to the first heterogeneous group of peaks, mainly in the range of 10 000–50 000 Da. The species corresponding to peak B was retained on the Microcon YM-50 filter (cutoff 50 000 Da), indicating the presence of oligomers with a molecular mass higher than 50 000 Da (Fig. 4B line 2 from the bottom). These data are in strong agree-

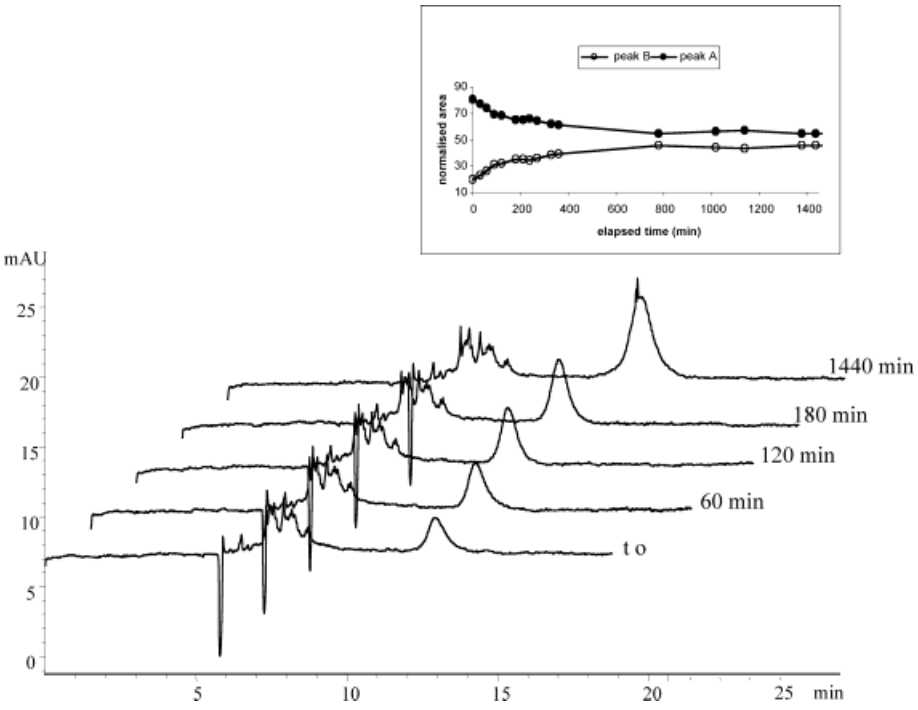

Figure 2. Electrophoretic profiles of Aβ 1-42 at different elapsed times from t_0. Experimental conditions are given in Section 2.3. Inset: Plot of the normalized area% [(peak area/ electrophoretic migration time) $\times$ 100]/ total area of peaks)] of the peak B and of the groups of peaks A *vs.* the different elapsed time (min).

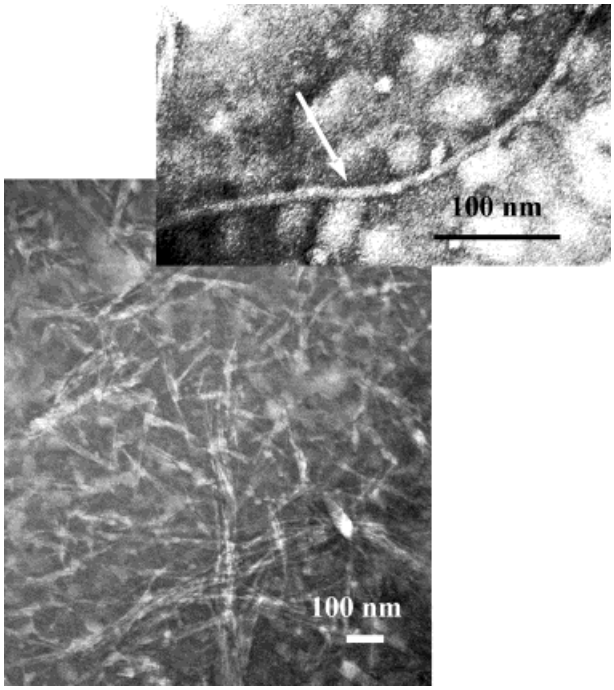

Figure 3. Electron micrograph of negatively stained samples exhibit nonbranched fibrils variously oriented presenting a medium diameter of 10 nm (scale bar: 100 nm). Inset: magnification of a single fibril (scale bar: 100 nm).

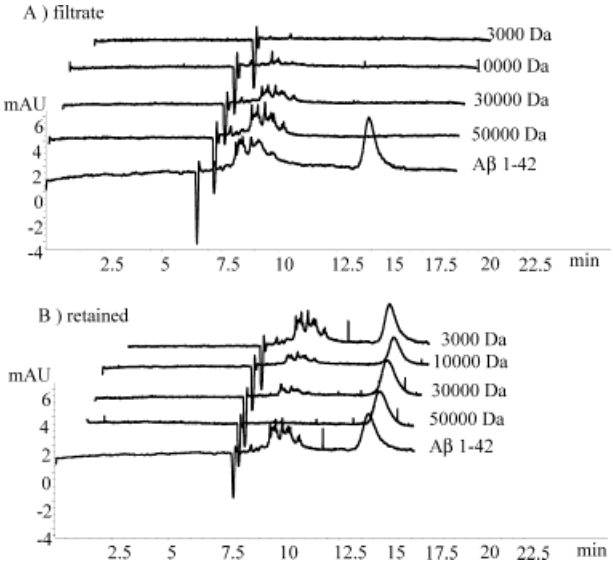

Figure 4. Electrophoretic profile of (A) Aβ 1-42 filtrate solutions and (B) Aβ 1-42 retained solutions immediately after solubilization by using different Microcon devices characterized by several cutoff (3000, 10 000, 30 000, 50 000 Da). Experimental conditions are given in Section 2.3.

ment with the hypothesis that the peak B characterized by a slower mobility corresponds to soluble oligomeric state of Aβ, presenting a molecular mass higher than 50 000 Da.

3.1.2 Aβ 1-40

The same investigations were carried out on Aβ 1-40 peptide. The electrophoretic profile of Aβ 1-40 at t_0 is shown in Fig. 5. The presence of one main peak (peak 3, $\mu_{eff} = -9.31 \times 10^{-5} \pm 6.67 \times 10^{-7}$; n=6) and of some small peaks (peaks 1, 2) was evidenced, whereas no peaks with comparable mobility to that of peak B of the electropherogram obtained by injecting Aβ 1-42 were detected. The electrophoretic patterns of Aβ 1-40 injected into the CE after different elapsed time from t_0 are shown in Fig. 6, where a progressive decrease of the area of peak 3 by increasing the elapsed time is observed. At 48 h after t_0 no peaks were detected by CE.

As for Aβ 1-42, Aβ 1-40 was ultrafiltrated through Microcon membranes characterized by different cut-off values. Both filtrated (Fig. 7A) and retained (Fig. 7B) solutions were analyzed and from the electrophoretic traces it is clear that peak 3 has a molecular mass between 10 000 and 30 000 Da. Notably the effective mobility of this peak stands within the mobility value window of the first group of peaks detected for Aβ 1-42 (from -4.17×10^{-5}

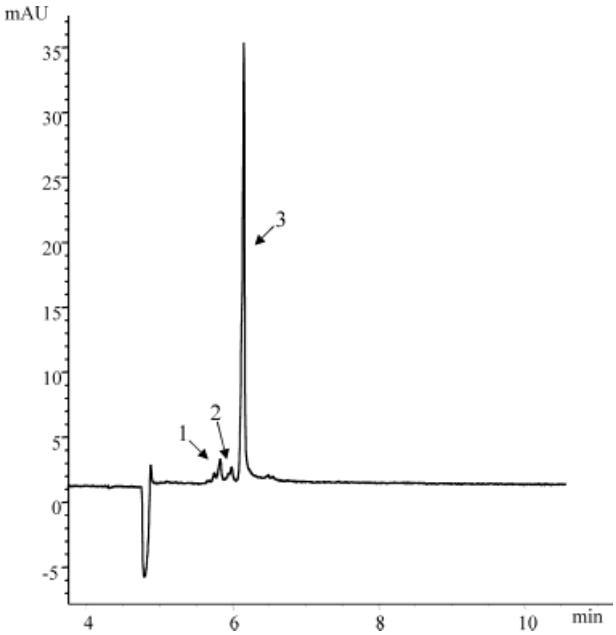

Figure 5. Electrophoretic profile of Aβ 1-40 immediately after supernatant withdrawal (t_0). Experimental conditions are given in Section 2.3.

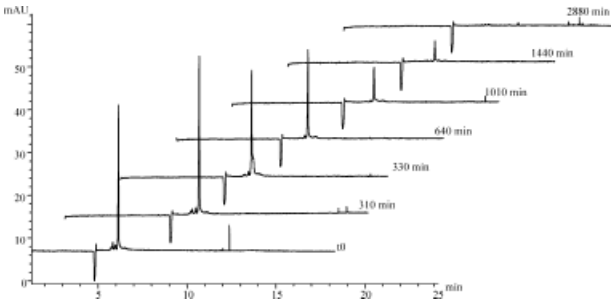

Figure 6. Electrophoretic profiles of Aβ 1-40 at different elapsed times from t_0. Experimental conditions are given in Section 2.3.

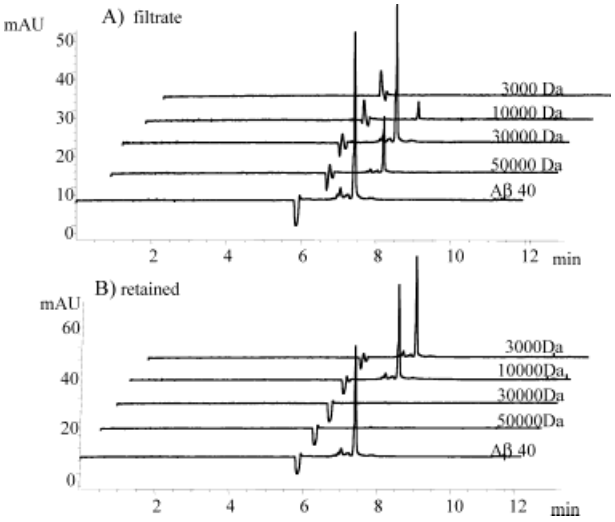

Figure 7. Electrophoretic profile of (A) Aβ 1-40 filtrate solutions and (B) Aβ 1-40 retained solutions immediately after solubilization by using different Microcon devices characterized by several cutoff (3000, 10 000, 30 000, 50 000 Da). Experimental conditions are given in Section 2.3.

$\pm 1.40 \times 10^{-6}$ to $-1.54 \times 10^{-4} \pm 1.14 \times 10^{-6}$; n=6) under the same electrophoretic conditions. Notwithstanding the known slower aggregation process for Aβ 1-40 when compared with Aβ 1-42 [21], the detection of a single and sharp peak is surprising, thus we further investigated the presence or the formation of different oligomeric species. This was accomplished by reducing the operative voltage and by varying the sample preparation procedure. A lowering in the operative voltage is intended to minimize, during the electrophoretic run, the potential disaggregating effect of high electric fields on formed aggregates. The effect of voltage on the three-dimensional (3-D) structure of proteins, and in particular on proteins presenting a high conformational plasticity has been previously reported, thus envisaging the possibility that the electric field could interfere with the noncovalent bonds that stabilize the 3-D structure [23, 24]. In this case, through a reduction of the voltage, we intended to rule out the possibility that the electric field could influence the strength of the noncovalent intermolecular interactions that sustain the peptide oligomerization. By using a shorter capillary (30 cm total length) and voltage values in the range of 1–16 kV (current= 4.5–99.5 μA), the profile of Aβ 1-40 peptide remained unchanged (data not shown).

As far as the effect of sample preparation, procedure B (see Section 2.2) was carried out with two aims: the use of fluorinated alcohols including HFIP would produce uniform, unaggregated monomers [14] by breaking down β-sheet structure and promoting α-helical secondary structure [25, 26]; acidic pH conditions would perturb the oligomerization process. Notwithstanding low pH values have been reported to favor fibrillogenesis for other amyloid-forming proteins [27, 28], structure formation of Aβ 1-40 with maintenance of solubility at pH below 3.5 has been published [29]. The same authors found that Aβ 1-40 at pH 7 forms an equilibrium of monomers and tetramers and that the presence of dimers cannot be ruled out.

Under both solubilization protocols (neutral and acidic pH) the electrophoretic traces remained unchanged (data not shown).

3.2 Cell toxicity experiments

In order to evaluate the biological role of the species separated by CE and ultrafiltration, cell toxicity experiments were carried out. The cellular model chosen is the neuroblastoma cell line (IMR32) which is sensitive to Aβ-induced cell death in a concentration-dependent manner. The standardization of our approach was accomplished by cell toxicity studies of the two peptides *in toto*. First we tested toxicity of Aβ 1-42 and we observed that exposure of IMR32 cells to 10 μM peptide induced a significant loss of cell viability (39.3% ± 4.74), (Fig. 8). Similar experiments were done on Aβ 1-40 and the exposure of IMR32 cells to 10 μM peptide for 24 h also resulted in a significant loss of cell viability (40.9% ± 1.62) (data not shown). Figure 8 also reports the cell toxicity played by the multimeric species of Aβ 1-42 retained on a filter with a cutoff of 50 000 Da and migrating at around 12 min in CE (peak B). Much lower toxicity is on the contrary to be assigned to Aβ 1-42 freely passing through a filter of 50 000 Da, and corresponding to the peptide fraction eluting in CE as group of peaks A.

4 Discussion

In the last few years enormous efforts have been generated from many disciplines to provide methods and technology able to describe the structure of the inter-

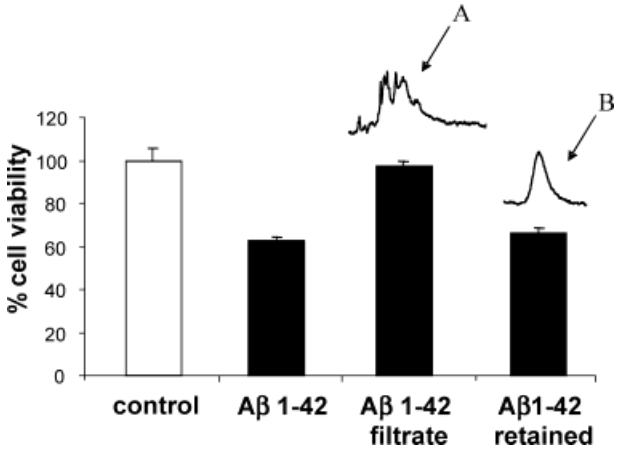

Figure 8. IMR32 cells were treated for 24 h with 10 μM Aβ peptide 1-42 and with its filtrate and the retained species. Cell viability, expressed as % of untreated cells, was determined by the MTT reduction assay.

converting conformers of Aβ protein along the fibrillogenesis pathway. Spectroscopic [7–12, 17, 29, 30], chromatographic [13, 30–33] and electrophoretic [14–17, 30, 33] techniques have provided several hints in the elucidation of the process. These techniques have been employed either alone or combined and nevertheless are not devoid of limitations or drawbacks, as clearly evidenced and reviewed by Bitan *et al.* [16, 17].

It is now largerly accepted that the initial phase of the aggregation implies a secondary structure transition and formation of small-size soluble oligomers [10, 12]. These early oligomers in the presence of a monomer reservoir undergo a further rearrangement and generation of paranuclei [5, 11] that seed the formation of fibrils [17]. Along the description of the fibrillogenic pathway more and more data are coming regarding the thermodynamic and kinetic barriers that regulate the transition from one state to the other [10] and regarding the biological role of Aβ fibrils, other efforts are devoted to the identification of the intermediate state of association that plays the cytotoxic activity.

CE offers in this context an orthogonal and advantageous approach to the already employed techniques as it merges simplicity, low consumption of precious Aβ peptides, high separation potential, speed of analysis, and furthermore makes it feasible a real and quantitative monitoring, in solution, of the aggregation process at plasma pH value. Most importantly we have carried out our *in vitro* studies of Aβ 1-42 and Aβ 1-40 without the use of chaotropic agents, and without the formation of covalent links.

The formation of cross-links [16, 17] offers the advantage to stabilize the various conformers but certainly would introduce modifications of the supersecondary structure as well as could affect the structural dynamics of the oligomers and in turn affect the biological behavior of the aggregate. The innovative purpose of this study in fact is the parallel monitoring of the process of Aβ aggregation and its influence on cell toxicity.

Aβ 1-42 presented an electrophoretic pattern characterized by a variety of peaks with a different mobility. It is reasonable to deduce that these peaks can be identified with different oligomeric species, occurring in an initial phase of the aggregation process. By using Microcon membranes to filter the peptide solution, we were able to assign an apparent molecular weight to the species related to the electrophoretic peaks. Considering that the molecular mass of the Aβ 1-42 monomer is 4514.15, we could conclude that by using CE, the first group of peaks corresponds to monomers up to undecamers, and can be significantly separated from a higher-molecular-weight species (peak B), that we identified as a dodecamer or an aggregate of larger size. Furthermore, by developing stability studies, we were able to observe that the area of peak B was increasing over time, at the expenses of the other species also present at t_0, which suggests that lower-size oligomers aggregate into higher size forms.

These data were consistent with the observation reported by Bitan *et al.* [17]. The oligomers Aβ 1-42, derived by the photo-induced cross-linking of unmodified proteins (PICUP) technique, were in fact characterized by a distinctly different oligomeric size distribution, spanning three main groups of oligomers, from monomers to trimers, from tetramers to octamers and from nonamers to dodecamers. This characterization is in agreement with the nucleation-elongation model related to the fibril formation, where species such as pentamers and hexamers represent units (paranuclei) which preferentially assemble to larger oligomers (dodecamers and high-molecular-weight species), which further precipitate as protofibrils and fibrils.

After identifying the high molecular weight-soluble oligomeric species that could be hypothesized to have a key role in the fibrillogenic process of Aβ 1-42, we have focused our attention on the effect of the freshly solubilized peptide and of this oligomeric species in a cellular system (IMR32 human neuroblastoma cells). IMR32 cell line is a cellular model vulnerable to Aβ peptide insult and it has been extensively used in our laboratory because it is sensitive to oxidative stress-induced cell death in a concentration-dependent manner. Consistent with the reports from literature, Aβ 1-42 presented a clear degree of toxicity [33, 34]. Moreover, it is also interesting to underline that the effect of the isolated species from Aβ 1-42 was different on IMR32 cells. While the species filtrated on Microcon YM-50 membrane (from dimers to decamers) did not induce cell death, the species retained from the 50 000 Da membranes (dodecamers and higher

aggregates) showed a toxicity similar to that observed when IMR32 cells were treated with the freshly dissolved Aβ 1-42, suggesting that peak B is an important intermediate of the pathogenetic aggregation pathway of this peptide. The aggregation pathway of the peptide may therefore include the formation of high-molecular-weight oligomeric species (peak B), which are fundamental in the development of toxicity. It is also demonstrated that more aggregated oligomeric species are more toxic than the smaller ones on the cells and that are strictly related to the greater toxicity of Aβ 1-42.

With the aim to compare the aggregation behavior of Aβ 1-42 and Aβ 1-40, the latter amyloidogenic peptide was studied and the electrophoretic profiles of Aβ 1-40 showed to be very different from those of Aβ 1-42, in the same experimental conditions. Notwithstanding the small difference in the primary structure between Aβ 1-40 and Aβ 1-42, we have constantly observed, under repeated injections of samples under the same conditions, only one main electrophoretic peak (peak 3) and two small faster peaks (peaks 1, 2). Neither at t_0 nor over elapsed time from withdrawal of the supernatant this pattern changed but rather the peak areas progressively decreased. This could indicate that Aβ 1-40 (M_r of the monomer 4328.9) features a different aggregation process, where in contrast to what observed for Aβ 1-42, seeds or nuclei characterized by high molecular weight are not formed.

Characterization studies by using Microcon membranes were carried out in order to support this hypothesis. According to the electropherograms shown in Fig. 7, this single peak should correspond to trimers up to eptamers, although a not negligible portion of peak 3 is filtrated by the Microcon YM-10 membrane (trace 2 from the top, Fig. 7A), suggesting the presence of dimers. The comigration of different oligomeric species in one single and efficient peak is nevertheless questionable. As mentioned earlier, for a peptide with such a high molecular flexibility, it is plausible that the high operating voltage may disrupt, during the electrophoretic process, unstable oligomers into lower-molecular-weight oligomers or monomers. For this reason, the lowest possible operative voltage value (1 kV) in CE was investigated, and under these conditions the electrophoretic pattern remained unchanged. The absence of direct voltage effect on the pattern of the electropherogram and the clear difference in the analysis of Aβ 1-40 and Aβ 1-42 are consistent with previous data suggesting a different pathway of the oligomerization process. In particular, by using CE, we were able to isolate a multimeric form of Aβ 1-42 presenting an apparent molecular mass higher than 50 000 Da and soluble up to several days. This approach could be therefore extremely useful in the investigation of the already established different fibrillogenic pathways of Aβ 1-40 and Aβ 1-42 [17]. The possibility to use CE in the study of these processes opens an avenue to evaluate the effect of different modulators of fibrillogenesis.

Supported by grants from Italian Ministry of Health (Progetto Finalizzato Alzheimer), and from the MIUR (PRIN 2003057355 and FIRB RBNEO1S29H).

Received April 1, 2004

5 References

[1] Dobson, C. M., *Trends Biochem. Sci.* 1999, *9*, 329–332.

[2] Merlini, G., Bellotti, V., *N. Engl. J. Med.* 2003, *349*, 583–596.

[3] Seubert, P., Vigo-Pelfrey, C., Esch, F., Lee, M., Dovey, H., Davis, D., Sinha, S., Schlossmacher, M. G., Whaley, J., Swindlehurst, C., McCormack, R., Wolfert, R., Selkoe, D. J., Lieberburg, I., Schenk, D.*Nature* 1992, *359*, 325–327.

[4] Shoji, M., Golde, T. E., Ghiso, J., Cheung, T. T., Estus, S., Shaffer, L. M., Cai, X., McKay, D. M., Tintner, R., Frangione, B., Younkin, S. G., *Science* 1992, *258*, 126–129.

[5] Hardy, J., Selkoe, D. J., *Science* 2002, *297*, 353–356.

[6] Klein, W. L., Krafft, G. A., Finch, C. E., *Trends Neurosci.* 2001, *24*, 219–224.

[7] Lambert, M. P., Barlow, A. K., Chromy, B. A., Edwards, C., Freed, R., Liosatos, M., Morgan, T. E., Rozovsky, I., Trommer, B., Viola, K. L., Wals, P., Zhang, C., Finch, C. E., Krafft, G. A., Klein, W. L., *Proc. Natl. Acad. Sci. USA* 1998, *95*, 6448–6453.

[8] Zagorsky, M. G., Shao, H., Ma, K., Yang, J., Li, H. Z., Zeng, H., Zhang, Y., Papolla, M., *Neurobiol. Aging* 2000, *21*, S10–S11.

[9] Crescenzi, O., Tomaselli, S., Guerrini, R., Salvadori, S., D'Ursi, A. M., Temussi, P. A., Picone, D., *Eur. J. Biochem.* 2002, *269*, 5642–5648.

[10] Kirkitadze, M. D., Condron, M. M., Teplow, D. B., *J. Mol. Biol.* 2001, *312*, 1103–1119.

[11] Lomakin, A., Teplow, D. B., Kirschner, A. D., Benedek, B. G., *Proc. Natl. Acad. Sci. USA* 1997, *94*, 7942–7947.

[12] Fezoui, Y., Teplow, D. B., *J. Biol. Chem.* 2002, *277*, 36948–36954.

[13] Roher, A. E., Chaney, M. O., Kuo, Y. M., Webster, S. D., Stine, W. B., Haverkamp, L. J., Woods, A. S., Cotter, R. J., Tuohy, J. M., Krafft, G. A., Bonnell, B. S., Emmerling, M. R., *J. Biol. Chem.* 1996, *271*, 20631–20635.

[14] Dahlgren, K. N., Manelli, A. M., Stine, W. B., Baker, L. K., Krafft, G. A., LaDu, M. J., *J. Biol. Chem.* 2002, *277*, 32046–32053.

[15] Stine, W. B., Dahlgren, K. N., Krafft, G. A., LaDu, M. J., *J. Biol. Chem.* 2003, *278*, 11612–11622.

[16] Bitan, G., Lomakin, A., Teplow, D. B., *J. Biol. Chem.* 2001, *276*, 35176–35184.

[17] Bitan, G., Kirkitadze, M. D., Lomakin, A., Vollers, S. S., Benedek, G. B., Teplow, D. B., *Proc. Natl. Acad. Sci. USA* 2003, *100*, 330–334.

[18] Varesio, E., Rudaz, S., Krause, K.-H., Veuthey, J.-L., *J. Chromatogr. A* 2002, *974*, 135–142.

[19] Thorsèn, G., Bergquist, J., Westlind-Danielsson, A., Josefsson, B., *Anal. Chem.* 2001, *73*, 2625–2631.

[20] Lloyd, D. K., Wätzig, H., *J. Chromatogr. B* 1995, *663*, 400–405.

[21] Jarret, J. T., Lansbury Jr., P. T., *Cell* 1993, *73*, 1055–1058.

[22] Ackermans, M. T., Everaerts, F. M., Beckers, J. L., *J. Chromatogr.* 1991, *549*, 345–355.

[23] Rochu, D., Pernet, T., Renault, F., Bon, C., Masson, P., *J. Chromatogr. A* 2001, *910*, 347–357.

[24] Rochu, D., Masson, P., *Electrophoresis* 2002, *23*, 189–192.

[25] Barrow, C. J., Zagorski, M. G., *Science* 1991, *253*, 179–182.

[26] Wood, S. J., Maleeff, B., Hart, T., Wetzel, R., *J. Mol. Biol.* 1996, *256*, 870–877.

[27] Bucciantini, M., Giannoni, E., Chiti, F., Baroni, F., Formigli, L., Zurdo, J., Taddei, N., Ramponi, G., Dobson, C. M., Stefani, M., *Nature* 2002, *416*, 507–511.

[28] Chiti, F., Bucciantini, M., Capanni, C., Taddei, N., Dobson, C. M., Stefani, M., *Prot. Sci.* 2001, *10*, 2541–2547.

[29] Jackson Huang, T. H., Yang, D.-S., Plaskos, N. P., Go, S., Yip, C. M., Fraser, P. E., Chakrabartty, A., *J. Mol. Biol.* 2000, *297*, 73–87.

[30] Walsh, D. M., Lomakin, A., Benedek, G. B., Condron, M. M., Teplow, D. B., *J. Biol. Chem.* 1997, *272*, 22364–22372.

[31] Hilbich, C., Kisters-Woike, B., Reed, J., Masters, C. L., Beyreuther, K., *J. Mol. Biol.* 1992, *228*, 460–473.

[32] Soreghan, B., Kosmoski, J., Glabe, C., *J. Biol. Chem.* 1994, *269*, 28551–28554.

[33] Chromy, B. A., Nowak, R. J., Lambert, M. P., Viola, K. L., Chang, L., Velasco, P. T., Jones, B. W., Fernandez, S. J., Lacor, P. N., Horowitz, P., Finch, C. E., Krafft, G. A., Klein, W. L., *Biochemistry* 2003, *42*, 12749–12760.

[34] Plant, L. D., Boyle, J. P., Smith, I. F., Peers, C., Pearson, H. A., *J. Neurosci.* 2003, *23*, 5531–5535.